Available online at www.sciencedirect.com
SCIENCE DIRECT
International Journal of Mass Spectrometry 249–250 (2006) 191–198
International Journal of Mass Spectrometry
www.elsevier.com/locate/ijms

Mechanisms of catalytic dehydrogenation of alkanes by rhodium clusters Rh_n^+ probed by isotope labelling

Christian Adlhart, Einar Uggerud *

Department of Chemistry, University of Oslo, P.O. Box 1033, Blindern, N-0315 Oslo, Norway

Received 31 October 2005; received in revised form 19 December 2005; accepted 20 December 2005
Available online 20 January 2006

Dedicated to the memory of Chava Lifshitz.

Abstract

The regioselectivity for the dehydrogenation of alkanes by rhodium clusters was investigated by reacting Rh_n^+, $n = 1$–20, with the isotopically labelled alkanes ethane-1,1,1-d_3 and propane-1,1,1,3,3,3-d_6. For Rh^+ reacting with propane a clear preference for a 1,2- over a 1,1- and 1,3-mechanism was observed. For larger clusters, hydrogen scrambling is faster than hydrogen elimination, which essentially leads to statistical formation of the neutrals H_2, HD, and D_2. Isotope scrambling with D_2 was also used as a structural probe for the reaction products of rhodium clusters with ethane. The intactness of the C–H bonds was demonstrated for ($n > 6$). The studies are completed with a detailed kinetic analysis for the reaction of Rh_7^+ with ethane and ethane/hydrogen and ethane/helium mixtures. An over-all picture with efficient C–H bond activation and fast and reversible hydrogen rearrangements emerges on the basis of these experiments. Some of the dehydrogenation reactions appear to be reversible.

Keywords: Rhodium cluster; Metal cluster; Ion molecule reaction; Nanotechnology; Catalysis; Deuterium labelling; Isotope effect; Reaction mechanism

1. Introduction

Catalytic dehydrogenation of alkanes to alkenes is an important process, which provides the feedstock for a large fraction of the polymer industry [1]. Since alkane dehydrogenation usually is a significantly endothermic process, the process requires either oxidation of the products, in particularly H_2, or the supply of thermal energy. It will be of great interest to better understand the mechanisms of dehydrogenations in general, and to suggest new catalysts for the industry in particular. In this respect, the study of gaseous transition metals and gaseous transition metal clusters is valuable [2–6]. Further insights are gained by directly comparing the behaviour of gaseous and supported atoms and clusters, as demonstrated for instance for rhodium in catalysing the trimerisation of acetylene [7]. Numerous experimental studies on rhodium cations [8–14] and rhodium clusters [15–17] as well as theoretical calculations [18–20] have aimed in understanding the principles for dehydrogenation of hydrocarbons, in particular alkanes. The metal clusters mimic essential features of catalyst surfaces. At the same time we also have to realize the differences. While a small gas phase metal cluster is an isolated system, metal clusters on a catalyst surface are in thermal contact with the solid support. While reaction products thermally desorb from a bulk surface, they have to be liberated from a gas phase cluster by activation (e.g., collisional activation). Despite the differences, gas phase cluster chemistry gives unique insights into important elementary reaction steps, including complications like cluster decomposition (reconstruction of the catalyst) and complete dehydrogenation (coking).

We have recently reported on the dehydrogenation of alkanes by cationic rhodium clusters [21]. Besides a surprising consistence in the cluster-size/reactivity pattern, it was also observed that dehydrogenation on gaseous rhodium clusters did not occur to completion, but for many reactions the generation of formal cluster-alkene adducts $(Rh_n,C_m,H_{2m})^+$ was observed. Our earlier experiments did neither reveal details about the structure of the alkene adducts nor their mechanism of generation. The thermodynamically most stable dehydrogenation products of propane and ethane are propene and ethene, respectively. Despite this, the actual mechanism for dehydrogenation is not necessarily via a 1,2-H_2 elimination mechanism. A preference of carbene binding to π binding may for example induce a shift in mechanism

* Corresponding author. Tel.: +47 22 85 55 37; fax: +47 22 85 54 41.
E-mail address: einar.uggerud@kjemi.uio.no (E. Uggerud).

1387-3806/$ – see front matter © 2006 Elsevier B.V. All rights reserved.
doi:10.1016/j.ijms.2005.12.032

from 1,2 to 1,1. The use of isotopically labelled molecules can provide these details.

In this context the principal issues are the structure of the intermediates and the regioselectivity of dehydrogenation. For atomic transition metal ions, regioselectivity is known to be strongly dependent on the nature of the metal, e.g., dominant 1,4-dehydrogenation for the reaction of Co^+ with *n*-butane in contrary to dominant 1,2-dehydrogenation for Rh^+ [9–11,22,23]. In case of metal clusters it may be possible that the mechanism of dehydrogenation is not only governed by the element, but also by the number of metal atoms. We have recently investigated the dehydrogenation of alkanes by rhodium clusters. While cationic rhodium clusters readily dehydrogenate higher alkanes, methane is less reactive. Without additional excitation, only Rh_2^+ and Rh_3^+ are capable of activating methane. The latter even requires the assistance of an inert chaperon such as argon to achieve the 1,1-dehydrogenation [16]. The reason for a higher reactivity of the higher alkanes compared to methane could either be due to a different mechanism or due to the possible formation of more stable alkene intermediates compared to carbene like species which is required in case of methane.

In this study, ethane-1,1,1-d_3 and propane-1,1,1,3,3,3-d_6 have been chosen as model substrates to probe the regioselectivity of dehydrogenation by rhodium clusters Rh_n^+, $n = 1$–20. In addition, isotope exchange experiments were performed to probe for the structure of reaction intermediates and for reversibility.

2. Experimental

The experiments were performed with a Fourier transform ion cyclotron resonance (FT-ICR) mass spectrometer, Bruker Apex 47e (Bruker Daltonics, MA, USA), with a supplementary source chamber with additional pumping attached to the standard source chamber. The experimental set-up is of the same design as used by Berg and co-workers, and has already been described thoroughly [21,24,25]. Thus, only a brief description of the operational techniques and conditions used in the present study will be given.

Rhodium cluster cations were generated by pulsed laser vaporisation of a rotating rhodium disk (99.9%, Goodfellow Cambridge Ltd., UK). A hot plasma was produced by focusing the second harmonic (532 nm) of a PL8020 Nd:YAG laser (Continuum, CA, USA, 20 Hz, 6–12 mJ per 5 ns pulse, focusing spot size 0.1–0.2 mm) on the target. The plasma was subsequently cooled and clustered by co-expansion with a short pulse of helium carrier gas through a confining channel (35, 2 mm i.d.). The helium gas (99.9999%, Aga, Norway) was introduced via a custom-built piezoelectric valve (20 μs opening time, backing pressure 30–40 bar). Both ions and neutrals are made in the process, making further ionisation unnecessary. The cluster ions were accelerated downstream from a 410 μm skimmer, transferred into the high field region of the 4.7 T superconducting magnet, decelerated and trapped in the ICR-cell. To increase the signal intensity, rhodium clusters were accumulated by 20 repetitive cluster generation and transfer cycles.

Hydrogen (99.97%, Aga, Norway), deuterium (99.998%, Hydro Gas, Norway), methane-d_4 (99 atom%, CDN Isotopes, Canada), ethane (99.9%, Aga, Norway), ethane-1,1,1-d_3 (99 atom%), propane-2,2-d_2 (99 atom%), and propane-1,1,1,3,3,3-d_6 (98 atom%, all Icon Isotopes, USA) were dispensed into the FT-ICR cell through a leak valve. During the experiments the pressure in the cell was raised from the base value of $\sim 3 \times 10^{-10}$ mbar to partial pressures of the hydrocarbons estimated to approximately 5×10^{-9} to 5×10^{-8} mbar. The substrate pressure was read out by means of a cold cathode ion gauge which was calibrated using the reaction of $NH_3^{\bullet+}$ (generated externally by EI) + $NH_3 \rightarrow NH_4^+ + NH_2^{\bullet}$, $k = 2.2 \times 10^{-9}$ cm^3 mol^{-1} s^{-1} [26] and corrected by relative sensitivity factors of $R(NH_3) = 1.12$, $R(He) = 0.37$, $R(H_2) = 0.59$, $R(CH_4) = 1.23$, $R(C_2H_6) = 1.91$, and $R(C_3H_8) = 2.56$ [27].

Reaction rates were determined directly from the total cluster distributions without prior isolation. The time dependent product ion distribution was obtained by recording mass spectra after a variable reaction time, t_r. Pseudo-first-order bimolecular rate constants for the total consumption of the rhodium cluster cations were taken from the slope of the straight lines obtained by plotting the natural logarithm of the normalized cluster ion intensities against t_r. The intensities were normalized against the total sum of ion intensities pertaining to each specific reactant cluster. Independent experiments with isolated cluster cations (correlated frequency sweeps [28] and in some cases additional single frequency shots) confirmed that there was no interference with potential decomposition products from larger clusters under the given experimental conditions. However, some decomposition products were observed at long reaction times (>60 s) and at high alkane pressures ($>2 \times 10^{-7}$ mbar). The major decomposition product was $Rh_2C_3^+$ irrespective of the carbon source, but the significant loss of ions from the cell under these conditions impedes a detailed analysis of the decomposition reaction [21].

The uncertainty of the absolute rates is typically ±40%, but relative rates are very precise. Errors are given at the 95% confidence level. For the determination of rate constants, reactions were observed until 90% consumption of the parent cluster ion. Relative partial rates for the primary products were determined by observing the reactions until 10% of secondary products (reaction with a second alkane) or oxidation products had formed and a simplified kinetic model with an average rate, k_{avg}, for the reaction rates of the primary to the secondary products was employed. The main difficulty for slow reactions was the competing reaction with molecular oxygen present in the background of the cell, which hampered the assignment of the reaction chronology for product clusters containing oxygen and hydrocarbon. Entries of slow reactions are therefore missing in Tables 1 and 2. Theoretical collisional rates were obtained using the parameterised model of Su and Chesnavich [29].

3. Results and discussion

As already mentioned, ethane dehydrogenation may occur via 1,2-elimination mechanism (Horiuti-Polanyi mechanism [30]) or a 1,1-elimination mechanism. This general situation is illustrated in Scheme 1. In principle each step may be reversible. The purpose of the present work is to probe to which extent this is true. For propane, the additional 1,3-elimination pathway may

Table 1
Reaction of Rh_n^+ with ethane-1,1,1-d_3

n	Two-fold dihydrogen loss				Single dihydrogen loss			
	$HD + D_2$ ($P(X_m) = 1/5$) [RE = 0.14]	$H_2 + D_2$ or 2HD ($P(X_m) = 3/5$) [RE = 0.02]	$HD + H_2$ ($P(X_m) = 1/5$) [RE = 0.14]	$\Phi(X_4)$ [RE = 0.02]	D_2 ($P(X_m) = 1/5$) [RE = 0.14]	HD ($P(X_m) = 3/5$) [RE = 0.02]	H_2 ($P(X_m) = 1/5$) [RE = 0.14]	$\Phi(X_2)$ [RE = 0.02]
1				0.04	0.33	0.59	0.08	0.96
2	0.12	0.26	0.62	0.58	0.34	0.35	0.31	0.42
3	0.24	0.36	0.40	0.95				0.05
4	0.31	0.18	0.51	0.33	0.36	0.28	0.36	0.67
7				0.10	0.16	0.22	0.62	0.90
8				0.27	0.22	0.26	0.52	0.73
9				0.85				0.15
10	0.35	0.30	0.35	0.84				0.16
11	0.34	0.27	0.39	0.95				0.05
12	0.41	0.27	0.32	0.95				0.05
13	0.38	0.26	0.36	0.93				0.07
14	0.40	0.27	0.33	0.92				0.08
16	0.34	0.21	0.45	0.55	0.46	0.31	0.23	0.45

Before normalisation, the neutral products distributions have been divided by $P(X_m)$, where $P(X_m)$ is the statistical probability for the formation of the neutral products H_2, HD, and D_2. $\Phi(X_m)$ is the relative partial rate between the product channels. Empty entries are due to an unfavourable branching in the primary reaction, which leads to both, a reduced signal to noise and an unambiguous assignment of secondary products, which could originate from both primary reaction channels. In case of the slowly reacting $Rh_{5,6,15,17-21}^+$, reaction with background oxygen was the dominant reaction channel, and their ambiguous reaction chronology impeded the determination of relative partial rates. RE is relative error (95%).

also be open. Analysis of the experimental data has to take these three limiting mechanisms for regioselectivity into account. Furthermore, hydrogen scrambling may also occur before the H_2 product is liberated. We envisage two fundamentally different scrambling mechanisms, illustrated in Schemes 1 and 2. It is obvious that initial C–H activation has to precede scrambling. Scheme 2 illustrates how scrambling may occur within the alkyl part of the alkyl hydride complex. Alternatively, scrambling may occur at the metal surface (Scheme 1). The latter situation requires a second C–H activation step and the formation of a dihydride intermediate. We do not reveal any details on adsorption states of ethene, which may either be π-bonded as found experimentally [31] or di-σ-bonded as found computationally [32].

3.1. Reaction with ethane-1,1,1-d_3

Results for the reaction of Rh_n^+, n = 1–20, with ethane-1,1,1-d_3 are presented in Table 1. The observed product distributions were corrected for the statistical probability of formation of the neutral products H_2, HD, and D_2 to simplify data interpretation. This was accomplished by dividing the corresponding ion abundance by the corresponding statistical probability, $P(X_m)$ (X = H or D). Thereafter, the data were normalized. Please note that in several cases there are sequential losses of two dihydrogens. In these cases corrections and normalisation had to be done within each dihydrogen loss in the sequence.

Results close to the statistically corrected and normalized 0.33:0.33:0.33 distribution are observed in a number of instances, as is evident from Table 1. This distribution would be the result of complete scrambling among the three hydrogen atoms and the three deuterium atoms. Alternatively, such a distribution is observable in a situation where 1,1- and 1,2-elimination occur at 40% and 60% probability (before statistical correction). We do of course not preclude this possible explanation, but it seems more likely that complete scrambling of hydrogen and deuterium before the irreversible elimination of X_2 from the cluster is the case here. It seems less likely that the chemically very different 1,1- and 1,2-elimination mechanism would give rise to identical rates for a majority of reactions. Table 1 also includes the relative partial rates, $\Phi(X_m)$, between single and two-fold dehydrogenation. These are in agreement with our earlier results [21].

Within experimental error, complete scrambling is observed for the majority of products. This is the case for the two-fold dehydrogenation by Rh_{10-14}^+ and the single dehydrogenation by Rh_2^+ and Rh_4^+. Apart from the majority of reactions, where formation of the neutral products has been observed at equal statistically corrected probability, there are some exceptions: notably, the single dehydrogenation of ethane by Rh^+. Here, HD elimination is with 59% clearly favoured over the expected 33% for complete scrambling. Two factors have to account for this observation: First, hydrogen elimination must be faster than the scrambling reaction and second, 1,2-eliminiation must be faster than 1,1-elimination. The latter is of significance, especially, since rhodium clusters do in general not react with methane. Dehydrogenation of methane would by necessity require the 1,1-elimination mechanism. A 1,1,-elimination is also essentially ruled out by the results for the reaction of propane, where the 1,2-elimination is preferred by a factor of ≈17 over the alternative 1,1- and 1,3-elimination (vide infra). We therefore conclude that most of the observed H_2 and D_2 losses come from scrambling (Schemes 1 and 2), rather than from specific 1,1-elimination.

There is a further feature in the Rh^+ result, which deserves consideration. In addition to the likelihood of scrambling, an isotope effect is in operation. This can be seen in the preference for loss of D_2 compared to H_2. This finding seems to be unexplained by the thermodynamics of the process, i.e., differences in

Table 2
Reaction of Rh_n^+ with propane-1,1,1,3,3,3-d_6

	Total dihydrogen loss		Three-fold dihydrogen loss				Two-fold dihydrogen loss				Single dihydrogen loss			
	H_2,D_6 ($P(X_m)=1$)	$\Phi(X_8)$ [RE = 0.02]	D_6 ($P(X_m)=1/28$) [RE = 0.48]	H,D_5 ($P(X_m)=12/28$) [RE = 0.02]	H_2,D_4 ($P(X_m)=15/28$) [RE = 0.02]	$\Phi(X_6)$ [RE = 0.02]	D_4 ($P(X_m)=6/28$) [RE = 0.04]	H, D_3 ($P(X_m)=16/28$) [RE = 0.02]	H_2,D_2 ($P(X_m)=6/28$) [RE = 0.04]	$\Phi(X_4)$ [RE = 0.02]	D_2 ($P(X_m)=15/28$) [RE = 0.02]	HD ($P(X_m)=12/28$) [RE = 0.02]	H_2 ($P(X_m)=1/28$) [RE = 0.48]	$\Phi(X_2)$ [RE = 0.02]
1											0.04	0.67	0.29	1.00
2							0.35	0.49	0.16	1.00				
3						0.02	0.24	0.62	0.15	0.98				
4							0.29	0.35	0.36	0.98				0.02
6											0.24	0.43	0.33	1.00
7							0.39	0.54	0.08	0.35	0.45	0.55	0.00	0.65
8						0.04	0.38	0.36	0.26	0.20	0.38	0.36	0.25	0.76
9						0.09	0.34	0.38	0.28	0.32	0.52	0.46	0.02	0.59
10			0.24		0.37	0.25	0.41	0.36	0.23	0.47	0.41	0.45	0.14	0.28
11	1.00	0.15	0.04	0.49	0.47	0.17	0.42	0.36	0.22	0.62				0.06
12		0.02	0.39	0.33	0.28	0.82	0.42	0.33	0.25	0.16				
13			0.30	0.38	0.32	0.53	0.41	0.32	0.27	0.47				
14			0.38	0.34	0.28	0.59	0.41	0.32	0.27	0.41				
15			0.40	0.34	0.27	0.24	0.43	0.32	0.25	0.76				
16			0.38	0.36	0.26	0.16	0.41	0.31	0.28	0.82				0.02
17						0.04	0.38	0.34	0.27	0.86				0.09
20		0.04				0.09	0.42	0.32	0.26	0.72				0.15

Before normalisation, the neutral products distributions have been divided by $P(X_m)$, where $P(X_m)$ is the statistical probability for the formation of the neutral products H_2, HD, and D_2. For multiple dihydrogen loss, we cannot distinguish between the different neutral products, e.g., 2HD or $H_2 + D_2$ for $\Delta m/z = -6$. $\Phi(X_m)$ is the relative partial rate between the product channels. Empty entries are due to an unfavourable branching in the primary reaction, which leads to both, a reduced signal to noise and an unambiguous assignment of secondary products, which could originate from both primary reaction channels. In case of the slowly reacting $Rh_{5,6,15,17\text{–}21}^+$, reaction with background oxygen was the dominant reaction channel, and their ambiguous reaction chronology impeded the determination of relative partial rates. RE is relative error (95%).

Scheme 1.

zero point vibrational energy. Assuming standard values of the frequencies of vibrations of C–H and H–H stretching and normal mass dependent isotope effects, simple calculation shows that H_2 loss requires 6 kJ mol^{-1} less than D_2 loss. Therefore, the kinetics are determining in this particular case, indicating that scrambling is slower than hydrogen elimination. For the sake of simplicity we now assume that the reaction follows the 1,2-elimination, Scheme 1, and that the 1,1-elimination rate is zero. Two scrambling mechanisms may be operative. While scrambling according to Scheme 1 is independent from a kinetic isotope effect – the transition state for C–H activation has to be passed for both, hydrogen and deuterium – scrambling accord-

Scheme 2.

ing to Scheme 2 depends on a kinetic isotope effect for the 1,2-shift. According to Scheme 2, scrambling and H_2 elimination require a 1,2-deuterium shift, whereas scrambling and D_2 elimination require a 1,2-hydrogen shift. The preferred D_2 elimination is then the result of the isotope effect in the 1,2-shift which is approximately $k_H/k_D = 4.1 \pm 1.9$ (calculated from the neutral product distributions of 0.33 and 0.08 in Table 1). Further equilibrium isotope effects and the possibility of a 1,1-elimination were neglected. This unique situation for Rh^+ compared to the larger clusters, where no isotope effect on hydrogen elimination is observed, is probably linked to the fact that the atomic metal atom only offers a single site for C–H activation, thereby giving quite strained transition structures. This reduces the rate for scrambling according to Scheme 1 relative to the other reaction steps, such that H_2, HD, or D_2 elimination occurs before scrambling has been complete.

Non-statistical behaviour in favour of H_2 + HD elimination is also observed for two-fold dehydrogenation on Rh_2^+. This is particularly interesting, since the statistical single dehydrogenation indicates, that scrambling has already been complete for the intermediate Rh_2,C_2,X_4^+. The non-statistical behaviour may then be a result of an isotope effect in the C–X activation steps which lead to a different kinetic preference of Rh_2,C_2,H_3,D^+ and Rh_2,C_2,H,D_3^+. The same preference, albeit less dominant, is observed for the two-fold dehydrogenation with Rh_3^+ and Rh_4^+.

The generally statistical behaviour observed for the reactions with the larger clusters appears to be due to a somewhat different mechanism compared to atomic rhodium. Having more active sites facilitates formation of a dihydride intermediate. The lifetime of the dihydride complexes is another important factor—the larger the cluster, the longer the lifetime. This will lead to a larger probability for scrambling before dihydrogen eliminates. Interestingly, Cox et al. observed an onset for the reaction between neutral rhodium clusters, Rh_n, and hydrogen at $n = 3$ with a large increase in reactivity for the next clusters in the series until the rates plateaued for $n \geq 5$ [33]. The reactivity of neutral and charged clusters can obviously not be compared directly, but for rhodium clusters $n \geq 18$ the geometry has been found to dominate over electronic effects [17].

3.2. Reaction with propane-1,1,1,3,3,3-d_6

The same principles as for the reaction with ethane-1,1,1-d_3 apply for the analysis of the reactions with propane-1,1,1,3,3,3-d_6. The results in Table 2 show complete scrambling for most of the larger clusters whereas there is one notable deviation for the reaction of Rh^+. The preference for HD over D_2 elimination enables us to distinguish between a 1,2- and a 1,1-mechanism or 1,3-mechanism. The latter has been reported for a large number of metal ions. For Rh^+, however, the 1,2-mechanism is favoured with 67% over 4%. The remaining 4% could still be the result of scrambling. For the sake of completeness, the numbers for a 2,2-elimination are shown in Table 2 as well, but the uncertainty in these numbers is too large to allow any firm conclusions.

In order to account for isotope effects, we also performed experiments with the alternatively labelled propane-2,2-d_2. Apart from the complication due to the overlapping Rh_n,C_3,H_2,D_2^+- and Rh_n,C_3,H_6^+-peaks, the results are identical within the experimental error to those obtained from the complementary labelled compound.

3.3. Reversibility of dehydrogenation?

Dehydrogenation of ethane:

$$C_2H_6 \rightarrow C_2H_4 + H_2$$

is endothermic. Despite this, dehydrogenation on metal clusters is observable when the generated C_2H_4 moiety becomes sufficiently strongly bonded to the cluster to overcome the endothermicity. In this way the overall reaction may be almost thermoneutral, and it is therefore of interest to see to which extent each elementary step is reversible, as indicated by default in Scheme 1. Although the overall dehydrogenation reaction could be reversible, it becomes efficiently irreversible under FT-ICR conditions where the pressure of hydrogen is zero. We therefore performed a series of kinetic experiments where the pressure of hydrogen was increased from 0 to 6.8×10^{-8} mbar while the partial pressure of ethane was kept constant at 1.0×10^{-8} mbar. The cluster Rh_7^+ was chosen for the experiments, because it has one of the highest fractions of Rh_n,C_2,H_4^+ as primary product. Time–intensity profiles for the reaction without hydrogen and with 3.4×10^{-8} mbar hydrogen are shown in Figs. 1 and 2. The reaction scheme depicted in Scheme 3 was found to be descriptive of the essential chemical reactions of the chosen rhodium/hydrocarbon cluster. It was used to set-up the reaction kinetics and to obtain reaction rates from numerical fits. The rate of the reverse reaction of I caused some problems in that respect, since its value was observed to fluctuate between +10% and −10% of the rate for I, when the hydrogen pressure was increased (vide infra). Since a negative rate is unphysical, it was set to zero for all the fits.

There are several notable features about Fig. 2 and Scheme 1: first, the peak intensity of $Rh_7H_2^+$ is time invariant. Due to leakage from hydrogen present in the FT-ICR cell into the source region, $Rh_7H_2^+$ is most likely already formed there. $Rh_7H_2^+$

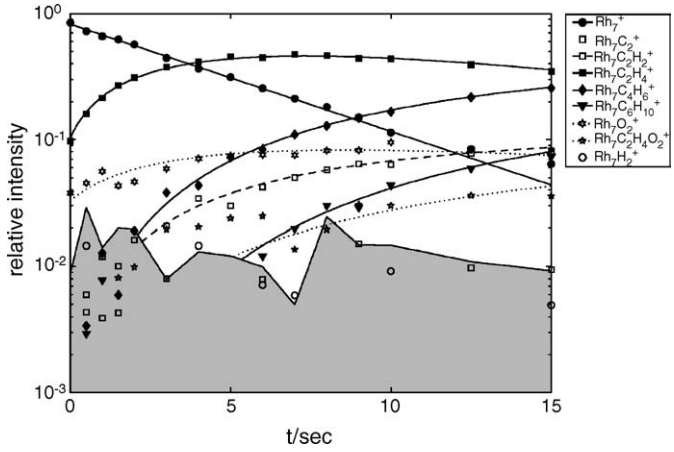

Fig. 1. Time–intensity profile for the reaction of Rh_7^+ with 1.0×10^{-8} mbar ethane. The shaded area indicates the noise level.

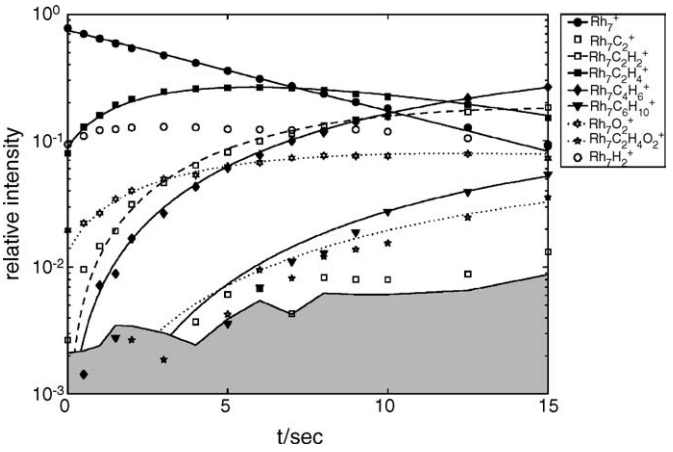

Fig. 2. Time–intensity profile for the reaction of Rh_7^+ with 1.0×10^{-8} mbar ethane and 3.4×10^{-8} mbar hydrogen. The reversibility of the reaction $Rh_7C_4H_6^+ \rightarrow Rh_7C_6H_{10}^+$ is illustrated in the parallel slope of the fit after 5 s. The shaded area indicates the noise level.

Table 3
Pseudo-first-order rates ($\times 10^{-10}$ cm^3 mol^{-1} s^{-1}) for the reaction of Rh_7^+ with ethane at different pressures ($\times 10^{-8}$ mbar) of hydrogen and helium according to Scheme 3

$p(C_2H_6)$	$p(H_2)$	p(He)	I	II	III	IV	V	VI	VIII
1.0	0.0	0.0	8.2	2.2	1.3	4.8	4.2	8.5	1.9
1.0	1.7	0.0	6.6	2.5	3.0	4.3	3.5	9.5 (5.8)	1.5
1.0	3.4	0.0	5.9	2.7	4.6	3.9	4.1	16.1 (5.0)	1.6
1.0	6.8	0.0	5.6	2.9	8.7	3.8	4.2	26.5 (4.0)	1.7
1.0	0.0	2.7	8.7	2.4	1.4	4.2	4.0	9.0	2.2
1.0	0.0	5.4	8.5	2.4	1.2	4.5	3.1	6.3	1.6
1.0	0.0	10.7	7.1	1.9	1.7	8.9	2.9	3.1	1.2

Rates marked as "slow" in Scheme 3 are not listed since they were below the detection limit, which is typically 10^{-11} cm^3 mol^{-1} s^{-1}. Absolute rates for reaction VII cannot be given, since the pressure of background oxygen is unknown. Values in parentheses: pseudo-first-order rates based on the partial pressure of H_2. The theoretical collision rate between Rh_7^+ and ethane is 9.16×10^{-10} cm^3 mol^{-1} s^{-1} [29].

does not take part in the reaction as was confirmed by separate isolation experiments. Second, Rh_7,C_2,H_2^+ is not formed by fast double dehydrogenation according to IX, as had been observed for RhC_2,H_2^+ [21], but is formed via the observable intermediate Rh_7,C_2,H_4^+. Third and most important, all single and double dehydrogenation reactions seem to be irreversible except for the reaction of Rh_7,C_4,H_6^+ with ethane, V.

Further observations are made, when the pressure of hydrogen is varied (Table 3 and Scheme 3). Most notable are the increased rates of reactions III and VI. Reaction VI is the reverse of the dehydrogenation reaction V and it would therefore be very clarifying to know whether the observed rate enhancement is due to a thermal effect, which could lead to an increased rate for ethene elimination, or if it is due to the actual reverse reaction (hydrogenation followed by ethane elimination). In order to distinguish between the two mechanisms the experiments were repeated with helium instead of hydrogen. Although the kinematics of collisional energy transfer between the clusters and hydrogen or helium are not identical, helium is still a good inert gas substitute: the theoretical collisional rate is half that of hydrogen, but with twice the amount of centre-of-mass collision energy. While the rate of VI increases in case of hydrogen, its rate is somewhat reduced in the presence of helium (Fig. 3, Table 3). This is a strong indication for a reverse hydrogenation rather than thermal dissociation of Rh_7,C_6,H_{10}^+. But a thermal dissociative component must also be present, since otherwise the rate of VI must be zero at a hydrogen pressure of zero.

The second observation made, when the pressure of hydrogen was varied was the rate enhancement of reaction III. We speculate that the C_2H_4 moiety in most of the Rh_7,C_2,H_4^+ ions has the wrong connectivity for further dehydrogenation to give Rh_7,C_2,H_2. Upon reaction with an H_2 molecule the necessary rearrangement may be accommodated: we have observed

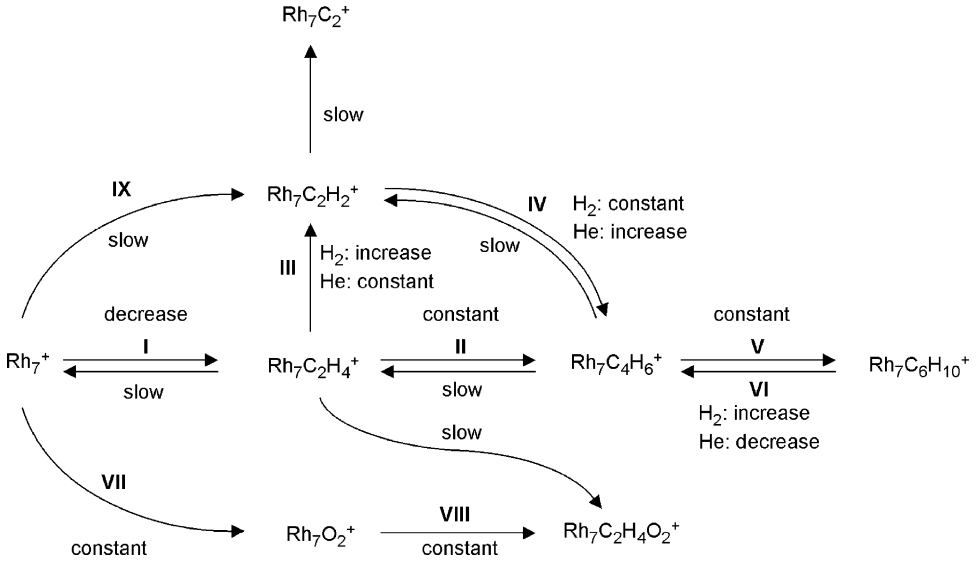

Scheme 3. Reaction scheme for the reaction of Rh_7^+ with ethane (background oxygen) and the variation of the fast reaction rates with increasing partial pressures of hydrogen and helium. The terms decrease/constant/increase are based on the rates are given in Table 3. "Slow" rates were below the detection limit, which is typically 10^{-11} cm^3 mol^{-1} s^{-1}.

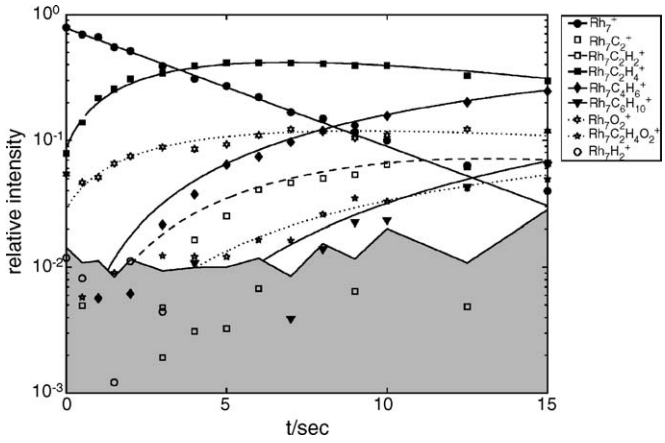

Fig. 3. Time–intensity profile for the reaction of Rh_7^+ with 1.0×10^{-8} mbar ethane and 5.4×10^{-8} mbar helium. The shaded area indicates the noise level.

kinetic preference for 1,2-elimination in the first dehydrogenation step (left hand route of Scheme 1) for Rh^+ and for the sake of the argument we may suppose that the same preference applies for the larger clusters. However, it is fully possible that a 1,1-elimination takes place. In general little is known about the structures of the intermediates. Some ideas can be obtained from computational studies of surface models and from spectroscopy of adsorbates on perfect surfaces. A thermodynamic preference for di-σ-bonded ethene to Rh(1 1 1) as well as Pt(1 1 1) surfaces has been inferred from density functional theory calculations for cluster models [32,34]. Infrared sum frequency generation experiments on the decomposition of ethene on Pt(1 1 1) surfaces revealed the formation of an ethylidyne (CCH_3) [35]. Formation of the ethylidyne can be achieved from the ethylidene ($CHCH_3$) intermediate. To the extent that the surface data applies to rhodium clusters, we propose that addition of the imposed H_2 molecule catalyses the rearrangement between Rh_7–(C_2H_4) (left-hand side of Scheme 1) and Rh_7–($CHCH_3$) on the right hand side through the alkyl hydride intermediate Rh_7–(H)(C_2H_5)$^+$. According to these speculations, the generation of a Rh_7,C_2,H_4^+ ion which has the correct connectivity for further dehydrogenation is catalysed by hydrogen and a rate enhancement for III with increasing hydrogen pressure is explained The interpretation of the enhanced rate for III due to the accessibility of the alkyl hydride intermediate Rh_7–(H)(C_2H_5)$^+$ is also consistent with experiments where helium instead of hydrogen was present and where no rate enhancements was observed (Table 3).

Based on reaction (Scheme 3) we have demonstrated that dehydrogenation of ethane by Rh_7^+ can be reversible under FT-ICR conditions by doing a kinetic analysis for the reaction of Rh_7^+ with ethane, ethane plus hydrogen, and ethane plus helium. However, the complexity of the reaction scheme makes the conclusions somewhat uncertain and alternative reaction schemes could, at least in principle, describe the experimental observations equally well. The ultimate distinction is not only hampered by the limited signal-to-noise level of our data, but also by the methodical difficulty that intermediates may have a different internal energies depending on how they are formed.

3.4. Exchange experiments with D_2

Exchange experiments with D_2 have previously been applied in the structural elucidation of the π-allyl hydride complex $HRhC_3H_5^+$ [36]. On the basis of the H_2 reaction experiments reported above, it appeared logical to extend the study to D_2 to see if this could reveal further structural and mechanistic features. Spectra were taken for a series of experiments with Rh_n^+, where the ethane pressure had been kept constant while the deuterium pressure was varied. Fig. 4 shows a typical example, Rh_7^+, with variable D_2 partial pressures between 0 and 5.7×10^{-8} mbar. It is clear that D exchanges with H, and that this is a sequential process.

Complete exchange occurs only for Rh_n,C_2,H_x^+ when $n > 6$. For $n = 3$ and 4 it is only partial within 12 s at $p(D_2) = 5.7 \times 10^{-8}$ and p(ethane) $= 0.9 \times 10^{-8}$ mbar. Exchange was not observed for $n < 3$. No results were obtained for $n = 5$ and 6, where oxidation through traces of background oxygen perturbed the identification of Rh_n,C_2,D_4^+, which has the same nominal mass as Rh_n,O_2^+.

It is fascinating to see how closely the exchange processes we notice in these experiments parallels the observation made before, that scrambling had almost been complete before dehydrogenation occurred. All this can be explained by assuming an intimate interplay between C–H and H–H activations exactly as illustrated in Scheme 1. Scheme 1 is not fully correct in the sense that not every step is reversible under all possible experimen-

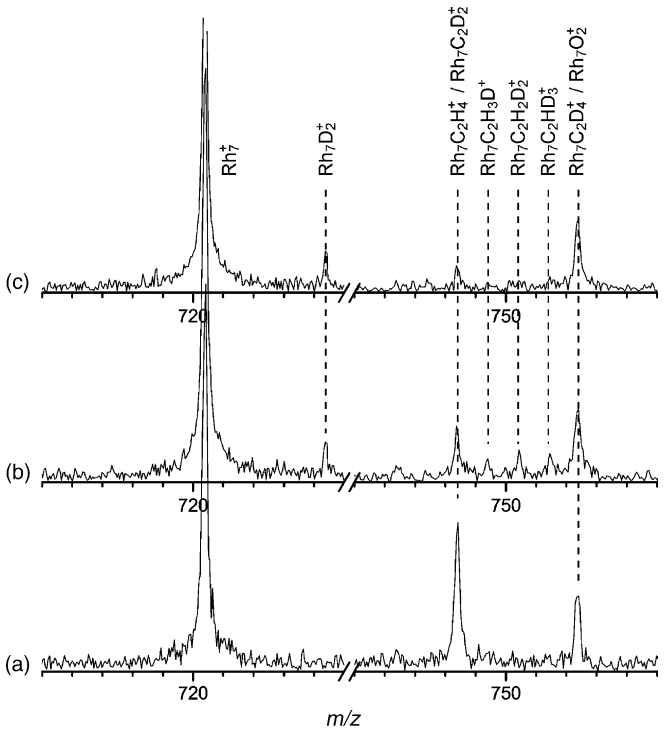

Fig. 4. Reaction of Rh_7^+ for 3 s with 0.9×10^{-8} mbar ethane and an increasing pressure of deuterium, panel (a). At 2.8×10^{-8} mbar deuterium, all Rh_7,C_2,H_x,D_y^+ peaks, $x + y = 4$, are observable, panel (b). At 5.7×10^{-8} mbar deuterium, scrambling is complete, panel (c). The peak at the nominal mass of Rh_7,C_2,H_4^+ is due to Rh_7,C_2,D_2^+. Rh_7,D_2^+ in the upper panels is already formed in the source region.

tal conditions. However, it remains clear that irrespective of the mechanism for hydrogen scrambling it is without any significant energy barrier.

Scheme 1 indicates that the C_2,H_4-unit could either be a doubly bonded carbene species, a π-bonded ethene, or an ethylene unit bounded to two different rhodium atoms through single bonds. Even further alternatives may exist, of which the most pertinent would be one where the C–C bond has been fully split. An intact C–C bond is not necessarily a precondition for deuterium scrambling, since scrambling has also been observed for platinum methylene clusters [37]. An experiment was designed to probe the possibility of a split C–C bond by adding CD_4 to the cell already containing ethane. However, no H/D exchange with CD_4 was observed as had been found in the reaction of $RhCD_2^+$ with CH_4 [8]. In principle this could have two different reasons; either the possible incapacity of rhodium clusters to activate the C–H bond in methane (methane is not dehydrogenated by "naked" rhodium clusters, $2 < n < 20$) or simply the absence of a methylene species, because the C–C bond within Rh_n,C_2,H_4^+ is intact.

Accordingly, we believe that the hydrogen atoms in Rh_7,C_2,H_2^+ are still attached to the carbon atom(s). However, we are not able to differentiate between intact and broken C–C bonds, where the two methylidyne units might eventually disproportionate into a methylene unit and a carbide.

The last observation concerns the lower limit for hydrogen scrambling which might be the result of a limited potency of the smaller rhodium clusters in stabilising a dihydride intermediate, which is required to initiate scrambling. The lack of small clusters to bind hydrogen is also observed in rate measurements by Cox [33]. The requirement of a hydride species is observed in the successful scrambling experiments with the hydride allyl complex $HRhC_3H_5^+$ whereas the anticipated butadiene complex, $RhC_4H_6^+$, however, remained untouched [36].

4. Conclusion

The reaction of cationic rhodium cluster with the isotopically labelled alkanes ethane-1,1,1-d_3 and propane-1,1,1,3,3,3-d_6 has been investigated and a clear regioselectivity for dehydrogenation is observed. For the reaction of monatomic rhodium cations with ethane, 1,2-elimination is preferred over the alternative 1,1-elimination. This observation is supported by the results with propane, where 1,2-elimination is at least 17 times faster the 1,1- and 1,3-elimination together. The ratio may even be larger, but an upper limit cannot be given due to abundant hydrogen scrambling, which becomes dominant for the larger rhodium clusters.

Isotope scrambling with D_2 was also used as a structural probe for the primary reaction products of rhodium clusters with ethane, Rh_n,C_2,H_x^+. While the integrity of the C–H bonds in these clusters was concluded from the specificity of the hydrogen exchange ($n > 6$), it remains unclear whether the C–C bond is intact. The observation of fast hydrogen scrambling also demonstrates the reversibility of the dehydrogenation reaction.

Chemical regeneration of Rh_7^+ from Rh_7,C_2,H_4^+ by hydrogenation was not observed, but Rh_7^+ can partly be recovered by collisional activation. Hydrogenation, however, was observed for the multiple coordinated Rh_7,C_6,H_{10}^+, where ethane could be eliminated through the reaction with hydrogen, whereas ethene was cleaved of thermally. The feasibility of the latter two reactions is an indication for a weaker bond between the C_2,H_4-unit and Rh_7,C_4,H_6^+ than between the C_2,H_4-unit and Rh_7^+.

References

[1] F. Bounomo, D. Sanfilippo, F. Trifirò, in: G. Ertl, H. Knözinger, J. Weitkamp (Eds.), Handbook of Heterogeneous Catalysis, VCH, Weinheim, 1997, p. 2140.
[2] P.B. Armentrout, Annu. Rev. Phys. Chem. 52 (2001) 423.
[3] D.C. Parent, S.L. Anderson, Chem. Rev. 92 (1992) 1541.
[4] M.P. Irion, Int. J. Mass Spectrom. Ion Proc. 121 (1992) 1.
[5] K. Eller, H. Schwarz:, Chem. Rev. 91 (1991) 1121.
[6] K. Bohme Diethard, H. Schwarz, Angew. Chem. Int. Ed. 44 (2005) 2336.
[7] K. Judai, A.S. Woerz, S. Abbet, J.-M. Antonietti, U. Heiz, A. Del Vitto, L. Giordano, G. Pacchioni, Phys. Chem. Chem. Phys. 7 (2005) 955.
[8] D.B. Jacobson, B.S. Freiser, J. Am. Chem. Soc. 107 (1985) 5870.
[9] M.A. Tolbert, J.L. Beauchamp, J. Am. Chem. Soc. 108 (1986) 7509.
[10] M.A. Hanratty, J.L. Beauchamp, A.J. Illies, M.T. Bowers, J. Am. Chem. Soc. 107 (1985) 1788.
[11] M.A. Tolbert, M.L. Mandich, L.F. Halle, J.L. Beauchamp, J. Am. Chem. Soc. 108 (1986) 5675.
[12] K.K. Irikura, J.L. Beauchamp, J. Phys. Chem. 95 (1991) 8344.
[13] Y.-M. Chen, P.B. Armentrout, J. Phys. Chem. 99 (1995) 10775.
[14] Y.-M. Chen, P.B. Armentrout, J. Am. Chem. Soc. 117 (1995) 9291.
[15] C. Berg, M. Beyer, T. Schindler, G. Niedner-Schatteburg, V.E. Bondybey, J. Chem. Phys. 104 (1996) 7940.
[16] G. Albert, C. Berg, M. Beyer, U. Achatz, S. Joos, G. Niedner-Schatteburg, V.E. Bondybey, Chem. Phys. Lett. 268 (1997) 235.
[17] C. Berg, M. Beyer, U. Achatz, S. Joos, G. Niedner-Schatteburg, V.E. Bondybey, J. Chem. Phys. 108 (1998) 5398.
[18] A. Kokalj, N. Bonini, C. Sbraccia, S. de Gironcoli, S. Baroni, J. Am. Chem. Soc. 126 (2004) 16732.
[19] J. Westerberg, M.R.A. Blomberg, J. Phys. Chem. A 102 (1998) 7303.
[20] D.L.S. Nieskens, A.P. van Bavel, D. Curulla Ferre, J.W. Niemantsverdriet, J. Phys. Chem. B 108 (2004) 14541.
[21] C. Adlhart, E. Uggerud, J. Chem. Phys. 123 (2005), 214709-1-10.
[22] R. Houriet, L.F. Halle, J.L. Beauchamp, Organometallics 2 (1983) 1818.
[23] D.B. Jacobson, B.S. Freiser, J. Am. Chem. Soc. 105 (1983) 5197.
[24] C. Berg, T. Schindler, G. Niedner-Schatteburg, V.E. Bondybey, J. Chem. Phys. 102 (1995) 4870.
[25] Å.M.L. Øiestad, E. Uggerud, Chem. Phys. 262 (2000) 169.
[26] Y. Ikezoe, S. Matsuoka, M. Takebe, A. Viggiano, Gas Phase Ion-Molecule Reaction Rate Constants through 1986, Maruzen, Tokyo, 1987.
[27] J.E. Bartmess, R.M. Georgiadis, Vacuum 33 (1983) 149.
[28] L.J. de Koning, N.M.M. Nibbering, S.L. van Orden, F.H. Laukien, Int. J. Mass Spectrom. Ion Proc. 165/166 (1997) 209.
[29] T. Su, W.J. Chesnavich, J. Chem. Phys. 76 (1982) 5183.
[30] J. Horiuchi, M. Polanyi, Trans. Faraday Soc. 30 (1934) 1164.
[31] C. Egawa, Surf. Sci. 454–456 (2000) 222.
[32] J. Kua, F. Faglioni, W.A. Goddard III, J. Am. Chem. Soc. 122 (2000) 2309.
[33] M.R. Zakin, D.M. Cox, A. Kaldor, J. Chem. Phys. 89 (1988) 1201.
[34] T. Jacob, W.A. Goddard III, J. Phys. Chem. B 109 (2005) 297.
[35] P. Cremer, C. Stanners, J.W. Niemantsverdriet, Y.R. Shen, G. Somorjai, Surf. Sci. 328 (1995) 111.
[36] G.D. Byrd, B.S. Freiser, J. Am. Chem. Soc. 104 (1982) 5944.
[37] C. Adlhart, E. Uggerud, unpublished results, 2005.